N-Hydroxyphthalimides and Metal Cocatalysts for the Autoxidation of *p*-Xylene to Terephthalic Acid

Basudeb Saha, Nobuyoshi Koshino, and James H. Espenson*

Ames Laboratory and Department of Chemistry, Iowa State University of Science and Technology, Ames, Iowa 50011

Received: June 30, 2003; In Final Form: November 11, 2003

N-Hydroxyphthalimide (NHPI) and its derivatives, such as 3-F-NHPI, 4-Me-NHPI, *N*-acetoxyphthalimide, and *N*,*N*-dihydroxypyromelitimide, were used as promoters with $Co(OAc)_2$ catalyst for the autoxidation of *p*-xylene (pX) and other methyl arenes. All the promoters gave acceptable rates and yields of terephthalic acid. The initial reaction rates, measured by the rate of oxygen uptake, were analyzed by a rate equation in terms of [pX], [Co(II)], and [NHPI]. The metal cocatalysts Mn(II) and Ce(III) accelerated the reaction significantly at millimolar concentrations. The reaction occurs by a chain mechanism that involves formation of the phthalimide *N*-oxyl radical, PINO• (that is, $R_2NO^•$), which abstracts a hydrogen atom from the methyl group of *p*-xylene to form the carbon-centered radical $ArCH_2^•$. In a stepwise fashion, the sequence progresses through alcohol, aldehyde, and carboxylic acid; at each stage, C−H abstraction by PINO• is involved. A significant kinetic isotope effect on the overall oxidation of *p*-xylene was found, $v_i(H)/v_i(D) = 3.4$. The activity of the substituted NHPI promoters follows the order NHPI > 3-F-NHPI > 4-Me-NHPI, which can be interpreted in terms of kinetic stability of the corresponding PINO radical.

Introduction

The catalytic oxidation of hydrocarbons by molecular oxygen is an important reaction for the production of commodity chemicals,[1,2] such as terephthalic acid, which is used to manufacture poly(ethylene terephthalate), a polymer commonly made into fibers, resins, films, etc. The most widely used catalyst package for the aerobic oxidation of *p*-xylene (pX) to terephthalic acid combines $Co(OAc)_2$, $Mn(OAc)_2$, and HBr.[3−7] Bromide, which corrodes expensive titanium reactors and forms $CH_3Br(g)$,[8] which can deplete the ozone layer, is, however, an undesirable component.[9,10]

Recently, Ishii et al.[11] have developed an efficient bromide-free catalyst package, which combines $Co(OAc)_2$ and *N*-hydroxyphthalimide (NHPI). This catalyst has been reported to be highly efficient for the aerobic oxidation of organic compounds containing sufficiently reactive C−H bonds, such as alkanes,[12] alkylbenzenes,[2] aromatic compounds containing benzylic groups,[13,14] and so on. The $Co(OAc)_2$/NHPI catalyst resembles the classical $Co(OAc)_2$/HBr combination that catalyzes oxidation of hydrocarbons in the sense, that under oxidative conditions, NHPI is converted to PINO•. Like the dibromide radical[15] formed from the bromide-containing system, the PINO radical abstracts a hydrogen atom from a C−H bond of the substrate and propagates radical chain branching.

The NHPI-based catalyst also offers the possibility that one may be able to tune the catalyst performance by introducing substituents on the aryl ring of the NHPI. In this study, we describe the kinetics of autoxidation of pX catalyzed by the combination of NHPI and $Co(OAc)_2$. The promoters investigated are shown in Chart 1. Kinetic studies have also been carried out in the presence of metal cocatalysts Mn(II) and Ce(III) to define their mechanistic roles.

CHART 1: Structural Formulas of Substituted *N*-Hydroxyphthalimides

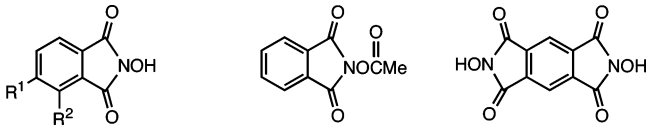

NHPI: $R^1 = R^2 = H$ NAPI NDHPI

3-F-NHPI: $R^1 = F$, $R^2 = H$

4-Me-NHPI: $R^1 = H$, $R^2 = Me$

Experimental Section

Reagents. The following materials were used as obtained commercially without purification: cobalt(II) acetate tetrahydrate, glacial acetic acid, NHPI, manganese(II) acetate, cerium(III) acetate, pX, pX-d_{10} (99+% D), *m*-xylene, pseudocumene, durene, *p*-toluic acid, 4-methylphthalic anhydride, 3-fluorophthalic anhydride, 1,2,4,5-benzenetetracarboxylic anhydride, hydroxylamine hydrochloride, and acetic anhydride.

The derivatives 4-Me-NHPI and 3-F-NHPI·H_2O were synthesized from the phthalic anhydrides and hydroxylamine hydrochloride according to a literature procedure.[16] The purity of each product was checked by ^1H NMR, and the observed values of the ^1H NMR parameters in DMSO-d_6 agreed with those reported.[16] Anal. Found (Calcd) for 4-Me-NHPI, $C_9H_7O_3N$: C, 60.19 (61.02); H, 3.89 (3.98); N, 8.28 (7.91). Anal. Found (Calcd) for 3-F-NHPI·H_2O, $C_8H_6FO_4N$: C, 48.21 (48.25); H, 2.86 (3.04); N, 6.89 (7.03).

N-Acetoxyphthalimide, NAPI, was prepared by dissolving NHPI (0.7 g, 4.2 mmol) in 10 mL of acetic anhydride and continuously stirring the mixture for 4 h. The solution was filtered to remove any insoluble NHPI, and the clear filtrate was allowed to cool in the refrigerator, whereupon NAPI

* Corresponding author.

10.1021/jp035870s CCC: $27.50
Published on Web 12/23/2003

precipitated as white crystals. ^{1}H NMR (δ, HOAc-d_4): 2.36 (C*H*$_3$, s); 7.84 (2H, d); 7.9 (2H, d). Anal. Found (Calcd) for $C_{10}H_7O_4N$: C, 58.43 (58.54); 3.09 (3.44); N, 7.40 (6.83).

N,*N*-Dihydroxypyromelitimide, NDHPI, was prepared from 1,2,4,5-benzenetetracarboxylic anhydride and hydroxylamine hydrochloride. The latter (1.34 g, 19.2 mmol) and Et_3N (2.6 mL, 19 mmol) were dissolved in 60 mL of ethanol. After the solution had been stirred for 10 min, 1,2,4,5-benzenetetracarboxylic anhydride (2.18 g, 9.8 mmol) was added. The mixture was refluxed for 8 h. As the reaction progressed, the clear solution gradually changed to yellow and then dark red. The resulting red solution was poured into ca. 100 mL of H_2O. The product precipitated as a yellow powder, which was filtered and dried under vacuum. Yield: 52%. ^{1}H NMR (δ, CD_3CN): 8.25 (2H, br s, NO*H*); 8.15 (2H, s). Anal. Calcd for $C_{10}H_4N_2O_6 \cdot 2H_2O$: C, 42.2; H, 2.84; N, 9.89. Found: C, 42.2; H, 2.88; N, 9.56.

A solution of $Co(OAc)_3$ in glacial acetic acid was prepared by passing ozone through a freshly prepared solution of $Co(OAc)_2 \cdot 4H_2O$.[17,18] Excess ozone was purged from the solution with a vigorous stream of argon. Cobalt(III) acetate exists in acetic acid in a number of forms,[19] but in these circumstances the species is the hydroxo-bridged dimetallic Co(III) complex known as $Co(III)_s$,[20] as confirmed by its characteristic UV−vis spectrum.[21]

General Procedure. The progress of the autoxidation reactions was monitored by the oxygen uptake method using a manometric apparatus similar to the one described in the literature.[1,22] The reactor, which contains an impeller to maintain oxygen saturation of the solution, was thermostated at 70 °C by means of a circulating water bath. Oxygen consumption was measured by monitoring the decrease in volume, at a constant 1 atm pressure of pure oxygen, in a buret connected to the reactor. The apparatus is shown in the Supporting Information. The initial reaction rates were calculated from the slope of the linear plots of the volume of oxygen consumption against time.

The oxidation products of some reactions were monitored by HPLC, having calibrated the method with known compounds, qualitatively and quantitatively. For these analyses, a 20 μL aliquot was removed from the reactor at different times during the reaction and diluted to 1 mL with 1:4 DMSO/CH_3CN (v/v). The diluted solution was then run through the HPLC column. A Waters model 501 solvent delivery system, Waters 996 photodiode array detector, and Novapak C_{18} 3.9 × 150 mm column were used for this method. A binary solvent of 50% H_2O/0.5% CH_3COOH and 50% CH_3CN with a flow rate of 0.7 mL/min was used in the isocratic mode. Identification of oxidation products was performed by comparing the retention time of the HPLC chromatogram peaks with those of authentic samples of *p*-tolualdehyde, *p*-toluic acid, 4-carboxybenzaldehyde, and terephthalic acid. Each peak in the HPLC chromatogram was properly integrated, and the actual concentration of each component was obtained from the precalibrated plot of peak area against concentration, as presented in Figure S1 in the Supporting Information.

Substituted PINO radicals were generated in glacial acetic acid by the oxidation of substituted NHPI with $Co(III)_s$:

$$R_2NOH + Co(OAc)_3 \rightarrow R_2NO^\bullet + Co(OAc)_2 + HOAc\ (k_f) \quad (1)$$

(In equations such as the one shown here, and others written subsequently, it is convenient to show stoichiometric formulas; ions are inappropriate in this low dielectric medium, and the full constitution of many metallic species has not been established.) The formation of PINO$^\bullet$ is accompanied by a large increase in absorbance in the vicinity of 380 nm. Values of the maximum wavelength and molar absorptivity are given in Table 1.

TABLE 1: Maximum Absorption Wavelengths and Molar Absorptivities for PINO$^\bullet$ in HOAc

radical	λ_{max}	ϵ^a
3-F-PINO$^\bullet$	367	1.35
PINO$^\bullet$	380	1.36
4-Me-PINO$^\bullet$	397	1.31

[a] Units 10^3 L mol^{-1} cm^{-1}.

The absorbance changes for formation and decomposition of these radicals were measured at 380 nm by UV−vis spectrophotometry, using Shimadzu UV-2101 and 2501 spectrophotometers. The absorbance−time data for the rapid formation reaction were to fitted to pseudo-first-order kinetics, eq 2. The subsequent self-decomposition step then set in, following second-order kinetics in accord with eq 3, where Y represents absorbance, k_ψ the pseudo-first-order rate constant for PINO$^\bullet$ formation, k_d the second-order rate constant for self-decomposition, and ϵ the molar absorptivity of PINO$^\bullet$.

$$Y_t = Y_\infty + (Y_0 - Y_\infty)e^{-k\psi t} \quad (2)$$

$$Y_t = Y_\infty + \frac{Y_0 - Y_\infty}{1 + (Y_0 - Y_\infty)k_d t/\epsilon} \quad (3)$$

Results

The overall oxidation of pX to terephthalic acid is given by the stoichiometry

$$C_6H_4(CH_3)_2 + 3O_2 \rightarrow C_6H_4(COOH)_2 + 2H_2O \quad (4)$$

Various partially oxidized forms of pX are produced during the course of the complex free radical chain reaction. One can use the oxygen uptake rate to monitor the reaction progress, but a cautionary note is in order: $-d[O_2]/dt = -3\ d[pX]/dt$ only in the limit in which the organic intermediates do not accumulate, which has not proved to be the case. Despite the numerical uncertainty so introduced, we have chosen to take the oxygen uptake rate as a convenient measure of the reaction rate. These intermediates may be 4-methylbenzyl alcohol, *p*-tolualdehyde, *p*-toluic acid, 4-carboxybenzyl alcohol, and 4-carboxybenzaldeyde.

Oxidation of pX with NHPI as Promoter. A preliminary study of the oxidation was carried out with 820 mM pX, 0.3 mM NHPI, and 40 mM $Co(OAc)_2$ in HOAc. The initial change in the volume of O_2 consumption was a linear function of time. The slope of the linear plot gives the initial reaction rate; when converted to concentration units, $v_i = 61.3 \times 10^{-6}$ mol L^{-1} s^{-1} as compared to 7.1×10^{-6} mol L^{-1} s^{-1} [22] with 10 mM NaBr in place of NHPI. Thus, the NHPI promoter is superior to bromide. However, the NHPI-promoted reaction almost stopped at ca. 1500 s, after consuming ca. 28 mL of O_2, which amounts to the oxidation of only 7% of pX conversion to *p*-tolualdehyde; by way of comparison, the bromide-promoted reaction resulted in ca. 1% pX oxidation in the same time. It was noticed that the NHPI reaction stopped as the solution took on a green color with a UV−vis spectrum that matched that of $Co(III)_s$. Further addition of 0.4 mM NHPI immediately turned the solution to a slightly darker pink color than that of the starting Co(II) solution. As shown in Figure 1, the reaction

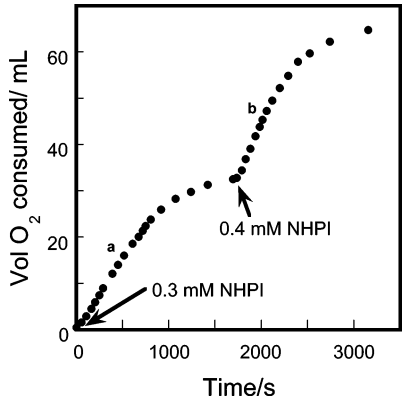

Figure 1. Volume of O_2 consumed as a function of time in an experiment with the following concentrations: 820 mM pX, 40 mM $Co(OAc)_2$, and (a) 0.3 mM or (b) an additional 0.4 mM NHPI at 70 °C in HOAc.

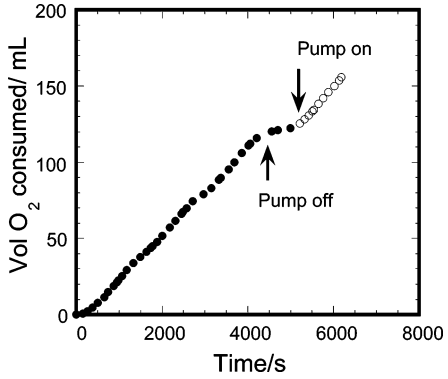

Figure 2. Volume of O_2 consumed as a function of time in an experiment utilizing a syringe pump to introduce a 20 mM NHPI solution at a flow rate of 0.82 mL/h. Other concentrations: 820 mM pX and 40 mM $Co(OAc)_2$ at 70 °C in HOAc.

resumed with $v_i = 83 \times 10^{-6}$ mol L^{-1} s^{-1}, but then stopped again after consuming another 30 mL of O_2 as $Co(III)_s$ again accumulated. Starting with a higher concentration of NHPI at the outset led to a reaction that stopped sooner.

From these results we concluded that small, continuous additions of NHPI might give better results. Thus, a syringe pump was used to deliver the NHPI solution into the reactor to test this idea. Two experiments were performed by injecting a stock NHPI solution (20 mM) into the reaction mixture containing 820 mM pX and 40 mM $Co(OAc)_2$ at 70 °C, at flow rates of 0.39 and 0.82 mL/h. As long as the NHPI solution was continuously added, in both cases the volume of O_2 was consumed linearly as a function of time, with v_i values of 26×10^{-6} and 57×10^{-6} M s^{-1}, respectively. However, the reaction stopped when the syringe pump was turned off, but started again when it was turned on. As shown in Figure 2, the reaction continued even after consuming 160 mL of O_2, a total of 1.24 mM NHPI having then been added. Without use of the syringe pump, the reaction stopped after consuming only 45 mL of O_2 when the 1.24 mM NHPI had been used.

Kinetics. Interestingly, at the low concentrations of Co(II), the reaction continued for a longer time, even without use of a syringe pump. An experiment under the conditions of 5 mM $Co(OAc)_2$, 5 mM NHPI, and 820 mM pX at 70 °C consumed 275 mL of O_2 in 2.5 h, which amounts to ca. 70% oxidation of pX to *p*-tolualdehyde. A series of such experiments was carried out, varying the concentrations of NHPI, Co(II), and pX in the ranges 1.0−7.9 mM, 5−25 mM, and 0.2−4.0 M, respectively. Table S1 shows the dependence of the initial reaction rates on

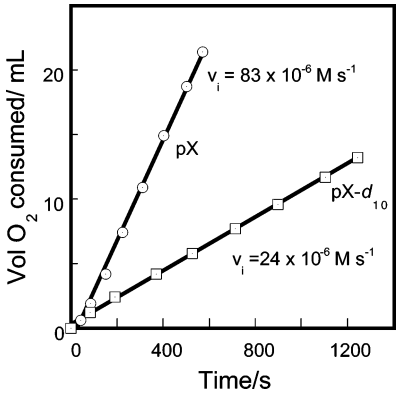

Figure 3. Dependence of v_i on the concentration of pX or pX-d_{10} under the conditions 820 mM pX, 40 mM $Co(OAc)_2$, and 0.4 mM [NHPI] at 70 °C in HOAc.

[NHPI], [Co(II)], and [pX]. From the series in which two of the three concentrations were held constant, the reaction is second-order with respect to both [Co(II)] and [pX], Figures S2 and S3, and first-order with respect to [NHPI], Figure S4. Combining those observations, we start to write $v = k[\mathrm{Co(II)}]^2[\mathrm{pX}]^2[\mathrm{NHPI}]$, but that did not fit the data.

A more elaborate form was used, which is actually in good accord with the kinetic equations for the scheme put forth by Zakharov.[23] This rate law, eq 5, where k_2, k_4, and k_H are the

$$-\frac{\mathrm{d[O_2]}}{\mathrm{d}t} = v = \frac{2\{k_2[\mathrm{pX}] + k_4[\mathrm{Co(II)}] + k_H[\mathrm{NHPI}]\}^2}{k_6} \quad (5)$$

second-order rate constants for the reaction of the peroxyl radical $ArCH_2OO^\bullet$ with pX, Co(II), and NHPI, respectively, is based on the free radical chain mechanism described in the Discussion. The second-order rate constant for the self-reaction of peroxyl radical, which is the termination step, is designated k_6.

Least-squares fitting of the 19 experimental data (Table S1) to eq 5, with k_6 fixed at 1.5×10^8 L mol^{-1} s^{-1},[24] gave $k_2 = 9.4 \pm 1.9$ L mol^{-1} s^{-1}, $k_4 = (2.5 \pm 0.1) \times 10^3$ L mol^{-1} s^{-1}, and $k_H = (7.1 \pm 0.3) \times 10^3$ L mol^{-1} s^{-1} at 70 °C. The experimental and fitted initial rates agree within ±18%. A comparison of experimental and fitted rates is given in Figure S5, which shows that the variations are random with respect to the concentration variables.

Kinetic Isotope Effects. The kinetic isotope effect (KIE) for the autoxidation of pX was measured by performing an experiment with 820 mM pX-d_{10}, 40 mM Co(II), and 0.4 mM NHPI. The result, as shown in Figure 3, yielded a significant KIE value: $v_i(H)/v_i(D) = 3.4 \pm 0.2$, which accounts for a hydrogen atom abstraction mechanism.

Different Substrates. Other methyl arenes, *m*-xylene, pseudocumene, and durene, were also studied with the $Co(OAc)_2$/NHPI combination, with 820 mM substrate, 40 mM $Co(OAc)_2$, and 0.4 mM NHPI. The initial reaction rates increased with the number of methyl groups. The results are summarized in Table 2. The rate differences are rather small, but perhaps the increase follows the order of the bond dissociation energies of the C−H bonds, which decreases from *m*-xylene to durene.

Oxidation of *p*-Toluic Acid. The intermediate product of the oxidation of pX with the Co(II)/NHPI catalyst is *p*-toluic acid. Once one methyl group of pX has been oxidized, the other methyl group is deactivated by the electron-withdrawing effect of the $-CO_2H$ group. Thus, the application of a catalyst in the manufacture of terephthalic acid depends on its effectiveness to oxidize *p*-toluic acid. To explore this further, *p*-toluic acid

TABLE 2: Initial Rates of Oxygen Uptake for the Autoxidation of 820 mM Methylarene, Catalyzed by 40 mM $Co(OAc)_2$ and 0.4 mM NHPI at 70 °C in HOAc

substrate	v_i[a]	v_1/n[b]	substrate	v_i[a]	v_1/n[b]
m-xylene	67	11	pseudocumene	93	16
p-xylene	83	14	durene	98	8.2

[a] Units 10^{-6} M s^{-1}; b = number of aliphatic hydrogen atoms (taken as 6 for pseudocumene).

TABLE 3: Comparison of the Initial Rates of O_2 Consumption Obtained from the NHPI- and Bromide-Promoted Autoxidation of pX under the Conditions 820 mM pX and 40 mM $Co(OAc)_2$ at 70 °C in HOAc

promoter (mM)	v_i[a]
NHPI (0.4)	20
Br^- (10)	1.9

[a] Units 10^{-6} M s^{-1}.

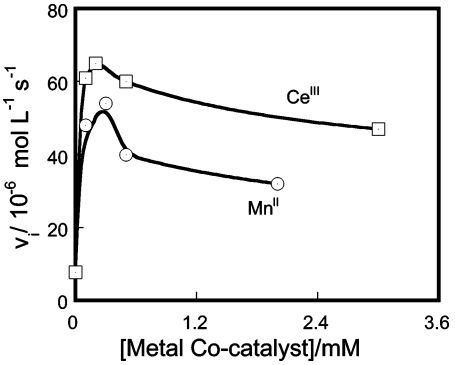

Figure 4. Dependence of the initial rates (v_i) of O_2 uptake for the Co(II)/NHPI-catalyzed autoxidation of pX on metal cocatalysts at 70 °C in HOAc.

was directly oxidized with the $Co(OAc)_2$/NHPI catalyst. A reaction with 820 mM substrate, 40 mM $Co(OAc)_2$, and 0.4 mM NHPI resulted in $v_i = 20 \times 10^{-6}$ mol L^{-1} s^{-1}. The same experiment with 10 mM NaBr in place of NHPI had $v_i = 1.9 \times 10^{-6}$ mol L^{-1} s^{-1}.[22] Thus, the efficiency of the NHPI-promoted oxidation of *p*-toluic acid is better than that of the bromide-promoted oxidation (Table 3).

Kinetic Effects of Metal Cocatalysts. The effectiveness of the $Co(OAc)_2$/NHPI catalyst was studied in the presence of a cocatalyst. $Mn(OAc)_2$, $Ce(OAc)_3$, and Zr(IV) (as a solution of zirconyl chloride in acetic acid) are known to accelerate reactions in which bromide[25,26] and bromoanthracene[22] are used to promote oxidation in a manner that shows strongly synergistic rate enhancements. The synergistic effects of $Mn(OAc)_2$ and $Ce(OAc)_3$ with the NHPI promoter are also quite significant. Experiments were performed at varying concentrations of metal cocatalysts, in the range of 0.1−2.0 mM for $Mn(OAc)_2$ and 0.1−3.0 mM for $Ce(OAc)_3$, with fixed concentrations of $Co(OAc)_2$ (5 mM), NHPI (1.0 mM), and pX (820 mM). The results are shown in Figure 4 and Table S2. In each case the rate attains a maximum value at a particular concentration of cocatalyst and then declines slowly. One experiment with 10 mM Zr(IV) showed no effect on the reaction rate.

Product Identification. HPLC determinations were performed on reactions starting with 100 mM pX, 5 mM $Co(OAc)_2$, 5 mM promoter, and the optimum concentration of $Mn(OAc)_2$ (0.3 mM) or $Ce(OAc)_3$ (0.15 mM). However, all reactions came to a halt after 42−50% of total oxidation due to decomposition of NHPI, which therefore was added at 5−7 mM concentration in one or two further portions. HPLC monitoring indicated that *p*-tolualdehyde was formed in the early stage, followed by 70−80% *p*-toluic acid in less than 1 h. The subsequent oxidation of *p*-toluic acid led to the formation of 4-carboxybenzaldehyde and then terephthalic acid. The formation of intermediate oxidation products and terephthalic acid as a function of time is shown in Figure S6. Figure 5 compares the yield of the final product, terephthalic acid, for different catalysts.

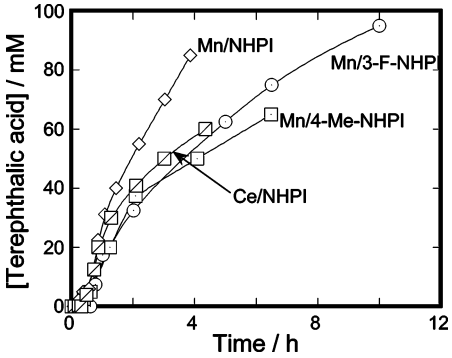

Figure 5. Yields of terephthalic acid formed from the autoxidation of 100 mM pX with the $Co(OAc)_2$ catalyst, NHPI promoters, and metal cocatalysts, 0.3 mM $Mn(OAc)_2$ or 0.15 mM $Ce(OAc)_3$ at 70 °C in HOAc.

Figure 5 illustrates a number of interesting features. First, the Co(II)/Mn(II)/NHPI catalyst is more efficient than the Co(II)/Ce(III)/NHPI catalyst in terms of yield of terephthalic acid. Second, the rate of formation of terephthalic acid with the unsubstituted NHPI is more effective than with the substituted one, the activity order being NHPI > 3-F-NHPI > 4-Me-NHPI. Under comparable conditions, an experiment with *p*-toluic acid as a starting substrate afforded a yield of 92% terephthalic acid in 3.5 h. The *p*-toluic acid oxidation, however, proceeded smoothly with the addition of 5 mM NHPI in one portion at the beginning of the reaction.

As mentioned above, pX oxidation stopped after 42−50% of total reaction with the combination of 5 mM substituted NHPI, 5 mM Co(II), and 0.3 mM Mn(II); it was therefore necessary to add more NHPI to complete the oxidation. Starting the reaction with the total amount of NHPI (10 mM) in one portion did not improve the yield either, except that the initial rate of O_2 consumption was higher. Cessation of the reaction after 42−50% may be due to the decomposition of NHPI. Decomposition of NHPI occurs rapidly during the oxidation of *p*-tolualdehyde to *p*-toluic acid, concurrently with the buildup of the green color of $Co(III)_s$. If the total quantity of NHPI used can be reduced by a simple modification, the present oxidation would be more desirable. In such efforts, the oxidation of pX was carried out with NAPI instead of NHPI. Under comparable conditions and at 70 °C, the reaction with NAPI was extremely slow, particularly in the first 20 h. However, complete oxidation to terephthalic acid was found using the NAPI in one portion at the beginning, without buildup of $Co(III)_s$. Moreover, the mother liquor of the first run was equally active for the second run, and was able to catalyze the oxidation of another 100 mM pX. The first and second runs produced 98% and 95% terephthalic acid in 70 and 74 h, respectively (Figure 6), the balance being *p*-toluic acid and 4-carboxybenzaldehyde.

NDHPI Promoter. This promoter contains two hydroxyimide moieties on the benzene ring. Therefore, we anticipated that it might be more active. Under comparable conditions 100 mM pX, 5 mM Co(II), 5 mM NDHPI, and 0.3 mM Mn(II) at 70 °C in HOAc, the beneficial effect of NDHPI was immediately realized from the initial reaction rate measurement, $v_i = 105 \times 10^{-6}$ mol L^{-1} s^{-1}, 33% higher than that of the NHPI-promoted oxidation. With a total of 6.5 mM NDHPI, the yield of

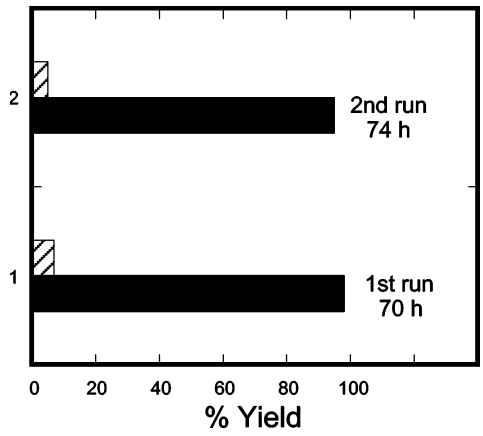

Figure 6. Yields of terephthalic acid (solid bar) and *p*-toluic acid (hatched bar) formed from the autoxidation of pX with 5 mM $Co(OAc)_2$, 0.3 mM $Mn(OAc)_2$, and 10 mM NAPI in both experiments at 70 °C in HOAc.

terephthalic acid was 85% in 4 h. As shown in Figure S6, the same reaction with the NHPI promoter required 10 mM NHPI to produce 85% terephthalic acid in 4 h. The beneficial effect of NDHPI has also been reported for the oxidation of nitrotoluenes.[27]

Discussion

Ishii et al. have reported a mechanism for the Co(II)/NHPI-catalyzed oxidation of methyl arenes.[11] It has been amply demonstrated that the metal-catalyzed autoxidations of methyl arenes are free radical chain reactions.[22,24,28] The initiator is the small concentration of an aralkyl hydroperoxide that is inevitably present in the hydrocarbon. The initiation step generates two reactive species, cobalt(III) and aralkoxyl radicals:

$$ArCH_2COOH + Co(OAc)_2 + HOAc \rightarrow ArCH_2O^{\bullet} + Co^{III}(OAc)_3 + H_2O \quad (6)$$

The highly reactive $ArCH_2O^{\bullet}$ then reacts with pX (here, $ArCH_3$) to form an aralkyl radical:

$$ArCH_2O^{\bullet} + ArCH_3 \rightarrow ArCH_2OH + ArCH_2^{\bullet} \quad (7)$$

As mentioned above, the aralkyl radical can also be formed in the following pair of reactions:

$$Co(OAc)_3 + R_2NOH \rightarrow Co(OAc)_2 + R_2NO^{\bullet} + HOAc \quad (8)$$

$$R_2NO^{\bullet} + ArCH_3 \rightarrow R_2NOH + ArCH_2^{\bullet} \quad (9)$$

The subsequent oxygenation of $ArCH_2^{\bullet}$ produces the important alkylperoxyl radical:

$$ArCH_2^{\bullet} + O_2 \rightarrow ArCH_2OO^{\bullet} \quad (10)$$

To justify the occurrence of reaction 8, independent studies of the reduction of $Co(III)_s$ with NHPI were carried out in HOAc at variable temperatures. $PINO^{\bullet}$ was formed quite rapidly, with $t_{1/2} = 33$ s for a reaction between 0.3 mM $Co(III)_s$ and 2.0 mM NHPI at 15 °C (Figure S7). The reaction between pX and $PINO^{\bullet}$, eq 9, exhibits a large KIE value, $k_H/k_D = 25.0$ at 25 °C.[29] Thus, the hydrogen abstraction in reaction 9 can be justified. Under the present catalytic condition, the KIE is $v_i(H)/v_i(D) = 3.4 \pm 0.2$, which indicates that the catalytic cycle also involves hydrogen abstraction, likely by the contributions from reactions 11 and 13, as given later.

The peroxyl radical formed from reaction 10 reacts with $ArCH_3$ and Co(II) to propagate and branch the radical chain reactions (eqs 11 and 12),[24,28] and a single peroxyl radical becomes three, by a sequence of pathways:

$$ArCH_2OO^{\bullet} + ArCH_3 \rightarrow ArCH_2OOH + ArCH_2^{\bullet} \ (k_2) \quad (11)$$

$$ArCH_2OO^{\bullet} + Co(OAc)_2 + HOAc \rightarrow ArCH_2OOH + Co(OAc)_3 \ (k_4) \quad (12)$$

The peroxyl radical can also abstract a hydrogen atom from the NHPI and participate in the chain-branching reactions:

$$ArCH_2OO^{\bullet} + R_2NOH \rightarrow ArCH_2OOH + R_2NO^{\bullet} \ (k_H) \quad (13)$$

The chain termination step is the self-reaction of the peroxyl radical by the Russell mechanism:[30]

$$2ArCH_2OO^{\bullet} \rightarrow ArCHO + ArCH_2OH + O_2 \ (k_6) \quad (14)$$

When the rates of chain branching and termination become equal, the concentration of the peroxyl radical and the steady-state oxidation rate can be expressed by eqs 15 and 16, respectively.

$$[ArCH_2OO^{\bullet}]_{ss} = \frac{k_2[ArCH_3] + k_4[Co(II)] + k_H[NHPI]}{k_6} \quad (15)$$

$$-\frac{d[O_2]}{dt} = v = \frac{2\{k_2[ArCH_3] + k_4[Co(II)] + k_H[NHPI]\}^2}{k_6} \quad (16)$$

Recently, Amorati et al.[31] reported the value of k_H as 7.2×10^3 L mol^{-1} s^{-1} at 30 °C in benzene for the autoxidation of cumene catalyzed by NHPI and 2,2′-azobis(2,4-dimethylvaleronitrile). The O−H BDE of NHPI in polar solvents is higher than that in non-hydrogen-bonding solvents such as benzene.[32,33] Therefore, the O−H BDE of NHPI can be expected to be larger in HOAc than in benzene; thus, k_H at 70 °C in HOAc seems reasonable. Zakharov et al. reported values of $k_2 = 4.5$ L mol^{-1} s^{-1} and $k_4 = 7.2 \times 10^2$ L mol^{-1} s^{-1} for the Co(II)/bromide-catalyzed autoxidation of pX at 70 °C.[24] Thus, our values of k_2 and k_4 are not in exact agreement, but each is within a factor of 2−3. The source of disagreement may be related to the accumulation of experimental error, with 3 parameters being determined from 14 data points.

As noted above, NHPI decomposition occurred during pX oxidation, particularly when O_2 was being consumed rapidly, indicative of a fast chain reaction. Consequently, $PINO^{\bullet}$ is also being formed quite rapidly, and it may suffer partial self-decomposition (Figure 7), in parallel with its involvement in the oxidation of substrates. Owing to the gradual decomposition of $PINO^{\bullet}$, the catalytic cycles become slower. Hence, the monomeric Co(III) generated in the chain reaction cannot reenter the catalytic cycle as efficiently given the net loss of NHPI. Thus, monomeric Co(III) gradually accumulates in the solution and then forms $Co(III)_s$.[19] Once fresh NHPI has been added, $PINO^{\bullet}$ is again generated in the reaction between $Co(III)_s$ and NHPI, and the catalytic cycle resumes.

Metal Cocatalysts. The roles of the redox-active metals Mn(II) and Ce(III) can be explained by their participation in the chain-branching mechanism, Scheme 1, similar to the one

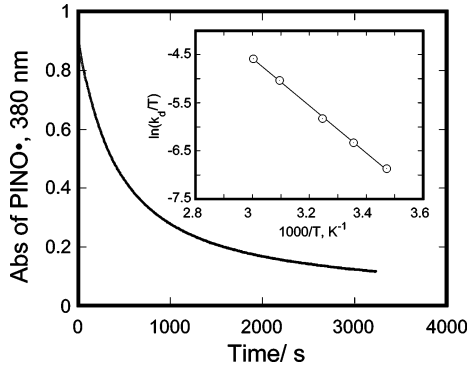

Figure 7. Decomposition of PINO radical generated from $Co(III)_s$ and NHPI at 60 °C in HOAc. Inset: $\ln(k_d/T)$ versus $1000/T$, giving $\Delta H^{\ddagger} = 40.7 \pm 0.6$ kJ mol^{-1} and $\Delta S^{\ddagger} = -109 \pm 2$ J K^{-1} mol^{-1}. k_d = second-order rate constant for self-decomposition of PINO•.

SCHEME 1: Chain Branching of Peroxyl Radicals in the Autoxidation of pX with Co(II)/NHPI

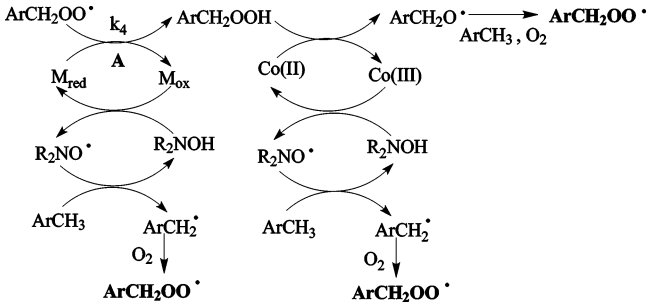

SCHEME 2: Inhibition of Chain Branching by Excess Mn(II)

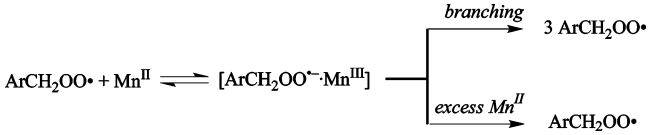

reported for the Co(II)/Mn(II)/bromide-catalyzed oxidation of pX.[18] The second-order rate constant for the step $ArCH_2OO^{\bullet}$ + Mn(II) is 10^3 times faster than the corresponding reaction with Co(II).[24] This can be explained by the lower reduction potentials of metal cocatalysts, 1.54 V for Mn(III/II) and 1.61 V for Ce(IV/III), compared with Co(III/II) (2.0 V).[34] Thus, in the presence of Mn(II) or Ce(III) step A of Scheme 1 becomes very fast, leading to rapid chain branching. Hence, $ArCH_2OO^{\bullet}$ is formed quickly. Step A with Mn(II) involves formation of an intermediate ion pair, $ArCH_2OO^{-}\cdot Mn^{III}$.[24] As shown in Scheme 2, the ion pair reacts with excess Mn(II), resulting in one $ArCH_2OO^{\bullet}$ instead of three. Therefore, the rate passes through a maximum at an optimal Mn(II) concentration.

Substituted NHPI Promoters. From Figure 5, the activities of substituted NHPI follow the order NHPI > 3-F-NHPI > 4-Me-NHPI. Wentzel et al.[16] reported the Co(II)/NHPI-catalyzed autoxidation of ethylbenzene. They suggested that 3-F-NHPI is most active, particularly at the initial stage of the reaction. The authors proposed a polar transition state between PINO• and substrate, where a partially negatively charged hydroxyl oxygen atom was stabilized by the electron-withdrawing F of 3-F-PINO. While such a polar transition state model does not support our experimental order of activity of substituted NHPI, we interpret our result in terms of the kinetic stability of the substituted PINO•.

To determine the kinetic stability of the PINO radicals, the rate constants for the formation of each type of radical[35] by Co(III) oxidation and its subsequent decomposition were determined. The results are as follows: (i) the formation of unsubstituted PINO• is faster than that of 4-Me-PINO•; (ii) the decomposition of unsubstituted PINO• is slower than its substituted analogues, increasing in the order PINO• < 3-F-PINO• < 4-Me-PINO•. Thus, it can be concluded that the kinetic stability, and hence the available concentration of each type of PINO• for the reaction with pX, follows the order PINO• > 3-F-PINO• > 4-Me-PINO•. This combination of reactivities explains our observed activity order.

The NAPI-promoted oxidation of pX is slower than that with NHPI, but NAPI remained active even after recycling. This can be explained by gradual hydrolysis of NAPI to the active form of promoter, NHPI, utilizing the water resulting from the oxidation. Therefore, NAPI is resistant to the rapid decomposition at an early stage of the reaction when the chain reaction takes place rapidly.

Acknowledgment. We are grateful for support from the National Science Foundation (Grant CHE-0240409) and BP Chemicals. This research was in part carried out at the facilities of the Ames Laboratory of the Office of Basic Energy Sciences, U.S. Department of Energy, under Contract W-7405-Eng-82 with the Iowa State University of Science and Technology.

Supporting Information Available: Tables showing the effects of reactant and catalyst concentrations and of cocatalysts on the initial rates of O_2 consumption, a diagram of the nanometric device for oxygen uptake measurements, a HPLC chromatogram of pX oxidation products, plots of initial rates of O_2 consumption versus concentration of reactant and catalysts, comparison of experimental and calculated initial rates of O_2 consumption, yields of oxidation products as a function of time, and formation of phthalimide *N*-oxyl radical. This material is available free of charge via the Internet at http://pubs.acs.org.

References and Notes

(1) Emanual, N. M.; Denisov, E. T.; Mazius, Z. K. *Liquid-Phase Oxidation of Hydrocarbons*; Plenum Press: New York, 1967; p 350.

(2) Yoshino, Y.; Hayashi, Y.; Iwahama, T.; Sakaguchi, S.; Ishii, Y. *J. Org. Chem.* **1997**, *62*, 6810−6813.

(3) Brill, W. F. *Ind. Eng. Chem.* **1960**, *52*, 837−840.

(4) Raghavendrachar, P.; Ramachandran, S. *Ind. Eng. Chem. Res.* **1992**, *31*, 453−462.

(5) Jacob, C. R.; Varkey, S. R.; Ratnasamy, P. *Appl. Catal., A* **1999**, *182*, 91−96.

(6) Cincotti, A.; Orru, R.; Cao, G. *Catal. Today* **1999**, *52*, 331−347.

(7) Partenheimer, W. *Catal. Today* **1995**, *23*, 69−157.

(8) Broeker, J. L.; Partenheimer, W.; Rosen, B. I. U.S. Patent No. 5453538, 1995.

(9) Environmental Protection Agency. *Fed. Regist.* **2003**, *68*.

(10) Li, C. M.; Hou, J.; Yu, Y.; Hou, H. *J. Environ. Sci.* **2000**, *12*, 266−269.

(11) Ishii, Y.; Sakaguchi, S.; Iwahama, T. *Adv. Synth. Catal.* **2001**, *343*, 393−427.

(12) Ishii, Y.; Iwahama, T.; Sakaguchi, S.; Nakayama, K.; Nishiyama, Y. *J. Org. Chem.* **1996**, *61*, 4520−4526.

(13) Ishii, Y.; Nakayama, K.; Takeno, M.; Sakaguchi, S.; Iwahama, T.; Nishiyama, Y. *J. Org. Chem.* **1995**, *60*, 3934−3935.

(14) Ishii, Y. *J. Mol. Catal. A* **1997**, *117*, 123−137.

(15) Metelski, P. D.; Espenson, J. H. *J. Phys. Chem. A* **2001**, *105*, 5881−5884.

(16) Wentzel, B. B.; Donners, M. P. J.; Alsters, P. L.; Feiters, M. C.; Nolte, R. J. M. *Tetrahedron* **2000**, *56*, 7797−7803.

(17) Jiao, X.; Espenson, J. H. *Inorg. Chem.* **2000**, *39*, 1549−1554.

(18) Metelski, P. D.; Adamian, V. A.; Espenson, J. H. *Inorg. Chem.* **2000**, *39*, 2434−2439 and references therein.

(19) Jones, G. H. *J. Chem. Res., Synop.* **1981**, 228−229.

(20) Chipperfield, J. R.; Lau, S.; Webster, D. E. *J. Mol. Catal.* **1992**, *75*, 123−128.
(21) Partenheimer, W.; Gipe, R. K. In *Nature of the cobalt-manganese-bromine catalyst in the methylaromatic compounds process*; Oyama, S. T., Hightower, J. W., Eds.; ACS Symposium Series; American Chemical Society: Washington, DC, 1993.
(22) Saha, B.; Espenson, J. H. *J. Mol. Catal. A* **2004**, *207*, 121−127.
(23) Zakharov, I. V.; Geletti, Y. V. *Petrol. Chem.* **1979**, *18*, 145−153.
(24) Zakharov, I. V. *Kinet. Catal.* **1998**, *39*, 523−532.
(25) Scientist: A Nonlinear Least-Squares Program, Version 2.01, MicroMath Scientific Software, Inc.
(26) Chester, A. W.; Scott, E. J. Y.; Landis, P. S. *J. Catal.* **1977**, *46*, 308−319.
(27) Sawatari, N.; Sakaguchi, S.; Ishii, Y. *Tetrahedron Lett.* **2003**, *44*, 2053−2056.
(28) Zakharov, I. V.; Geletii, Y. V.; Adamian, V. A. *Kinet. Catal.* **1991**, *32*, 31−37.
(29) Koshino, N.; Saha, B.; Espenson, J. H. *J. Org. Chem.*, accepted for publication.
(30) Russell, G. A. *J. Am. Chem. Soc.* **1957**, *79*, 3871−3877.
(31) Amorati, R.; Lucarini, M.; Mugnaini, V.; Pedulli, G. F.; Minisci, F.; Recupero, F.; Fontana, F.; Astolfi, P.; Greci, L. *J. Org. Chem.* **2003**, *68*, 1747−1754.
(32) Amorati et al. have estimated the O−H BDE as 369 and 364 kJ/mol in *t*-BuOH and in non-hydrogen-bonding solvents. The estimated BDE in DMSO is even larger, 375 kJ/mol (ref 31).
(33) Koshino, N.; Cai, Y.; Espenson, J. H. *J. Phys. Chem. A* **2003**, *107*, 4262−4267.
(34) Adamian, V. A. Private communication, as cited in ref 18.
(35) Cai, Y.; Koshino, N.; Saha, B.; Espenson, J. H. Manuscript in preparation.